Parkinsonism and Related Disorders 61 (2019) 179–186

Contents lists available at ScienceDirect

Parkinsonism and Related Disorders

journal homepage: www.elsevier.com/locate/parkreldis

PLA2G6-associated neurodegeneration: New insights into brain abnormalities and disease progression

Alejandra Darling[a,1], Sergio Aguilera-Albesa[b,1], Cristina Aisha Tello[c], Mercedes Serrano[d], Miguel Tomás[e], Rafael Camino-León[f], Joaquín Fernández-Ramos[f], Adriano Jiménez-Escrig[g], Pilar Poó[a], Mar O'Callaghan[a], Carlos Ortez[a], Andrés Nascimento[a], Ramón Candau Fernández Mesaque[h], Marcos Madruga[h], Luisa Arrabal[i], Susana Roldan[i], Hilario Gómez-Martín[j], Cristina Garrido[k], Teresa Temudo[k], Cristina Jou-Muñoz[l], Jordi Muchart[m], Thierry A.G.M. Huisman[n], Andrea Poretti[n], Vincenzo Lupo[c], Carmen Espinós[c], Belén Pérez-Dueñas[a,o,*]

[a] Pediatric Neurology Department, Hospital Sant Joan de Déu, University of Barcelona, Barcelona, Spain
[b] Pediatric Neurology Unit, Department of Pediatrics, Complejo Hospitalario de Navarra, Navarrabiomed, Pamplona, Spain
[c] Unit of Genetics and Genomics of Neuromuscular and Neurodegenerative Disorders, Centro de Investigación Príncipe Felipe, Valencia, Spain
[d] Neurology Department, Hospital Sant Joan de Déu, University of Barcelona, Barcelona, CIBERER, Instituto de Salud Carlos III, Spain
[e] Pediatric Neurology Department, Hospital Universitario Politécnico La Fe, Valencia, Spain
[f] Pediatric Neurology Department, Hospital Universitario Reina Sofía, Córdoba, Spain
[g] Neurology Department, Hospital Ramón y Cajal, Madrid, Spain
[h] Pediatric Neurology Department, Hospital Universitario Virgen del Rocío, Sevilla, Spain
[i] Pediatric Neurology Department, Hospital Virgen de las Nieves, Granada, Spain
[j] Pediatric Neurology Department, Hospital San Pedro de Alcántara, Complejo Hospitalario Universitario de Cáceres, Spain
[k] Pediatric Neurology Department, Centro Materno-Infantil, Centro Hospitalario do Porto, Porto, Portugal
[l] Pathology Department, Sant Joan de Déu Hospital, University of Barcelona, Barcelona, CIBERER, Instituto de Salud Carlos III, Spain
[m] Neuroradiology Department, Sant Joan de Déu Hospital, University of Barcelona, Barcelona, Spain
[n] Division of Pediatric Radiology and Pediatric Neuroradiology, Russell H. Morgan Department of Radiology and Radiological Science, The Johns Hopkins University School of Medicine, Baltimore, MD, USA
[o] Pediatric Neurology Research Group, Vall d'Hebron Research Institute (VHIR), Universitat Autònoma de Barcelona, Barcelona, Catalonia, Spain

ARTICLE INFO

Keywords:
PLA2G6-gene
PLA2G6-associated neurodegeneration (PLAN)
Infantile neuroaxonal dystrophy
Infantile PLAN
atypical neuroaxonal dystrophy
Childhood PLAN
Magnetic resonance imaging (MRI)
Neurodegeneration with brain iron accumulation (NBIA)

ABSTRACT

Introduction: *PLA2G6*-associated neurodegeneration (PLAN) comprises a continuum of three phenotypes with overlapping clinical and radiologic features.

Methods: Observational clinical study in a cohort of infantile and childhood onset PLAN patients and genetic analysis of the *PLA2G6* gene. We analysed chronological evolution in terms of age at onset and disease course through a 66-item questionnaire. We performed qualitative and quantitative assessment of MRI abnormalities and searched for clinical and radiological phenotype and genotype correlations.

Results: Sixteen PLAN patients (mean age: 10.2 years, range 3–33) were evaluated, with a median onset (years) of signs/symptoms as follows: neurological regression (1.5), oculomotor abnormalities (1.5), hypotonia (1.8), gait loss (2.2), pyramidal signs (3.0), axonal neuropathy (3.0), dysphagia (4.0), optic atrophy (4.0), psychiatric symptoms (4.0), seizures (5.9), joint contractures (6.0), dystonia (8.0), bladder dysfunction (13.0) and parkinsonism (15.0). MRI assessment identified cerebellar atrophy (19/19), brain iron deposition (10/19), clava hypertrophy (8/19) and T2/FLAIR hyperintensity of the cerebellar cortex (6/19). The mid-sagittal vermis relative diameter (MVRD) correlated with age at onset of clinical variants, meaning that the earlier the onset, the more severe the cerebellar atrophy. All patients harboured missense, nonsense and frameshift mutations in *PLA2G6*, including four novel variants.

Conclusions: Cerebellar atrophy was a universal radiological sign in infantile and childhood onset PLAN, and

* Corresponding author. Paediatric Neurology Research Group, Vall d'Hebron Research Institute (VHIR), Universitat Autònoma de Barcelona. Passeig de la Vall d'Hebron, 119-129, 08035, Barcelona, Catalonia, Spain.
E-mail address: belen.perez@vhir.org (B. Pérez-Dueñas).
[1] These authors contributed equally.

https://doi.org/10.1016/j.parkreldis.2018.10.013
Received 11 May 2018; Received in revised form 19 September 2018; Accepted 12 October 2018

correlated with the severity of the phenotype. Iron accumulation within the globus pallidum and substantia nigra was also a common and strikingly uniform feature regardless of the phenotype.

1. Introduction

Phospholipase A2 Group VI (*PLA2G6*)-associated neurodegeneration (PLAN) is the second most frequent form among neurodegeneration with brain iron accumulation (NBIA) disorders [1]. PLAN encompasses a continuum of three overlapping phenotypes: infantile-onset PLAN, corresponding to classic infantile neuroaxonal dystrophy (INAD) (MIM#256600), childhood-onset PLAN corresponding to atypical neuroaxonal dystrophy (ANAD) (MIM#610217) and juvenile-adult-onset PLAN corresponding to *PLA2G6*-related dystonia-parkinsonism (MIM#612953) [2,3]. Moreover, new cases are increasingly reported, and the phenotypic spectrum is expanding, including hereditary spastic paraplegia with brain iron accumulation [4,5].

PLAN is an autosomal recessive disorder caused by mutations in the *PLA2G6* gene (MIM*603604) [6]. This gene encodes a calcium-independent phospholipase A2 enzyme (iPLA2-VI) with key functions in maintaining cell membrane homeostasis, through phospholipid remodelling [2,6,7]. Pathologically, PLAN is characterised by the depletion of cerebellar cortical neurons accompanied by astrocytosis, axonal spheroids in the central and peripheral nervous system and progressive brain iron deposition [2,8]. Cerebellar atrophy is often the earliest sign on magnetic resonance imaging (MRI), whilst evidence of brain iron deposition in the basal ganglia appears later [2,9]. In the dystonia-parkinsonism phenotype, brain iron accumulation has been reported in one third of the patients [10].

In the present study, we genotyped patients with PLAN, performed a standardised neurological examination and assess the chronological evolution of the main signs and symptoms of the disease. Second, we completed a qualitative and quantitative assessment of brain MRI abnormalities and reviewed previously published neuroradiological studies. Analysis of clinical, radiological and genetic findings allowed us to demonstrate significant correlations between the severity of the disease and the degree of cerebellar atrophy, which was a constant neuroimaging feature in our series. Also, we identified a set of patients with null mutations and a more severe clinical and radiological phenotype. Finally, we described novel *PLA2G6* variants, further expanding the current knowledge on genetics in PLAN.

2. Methods

2.1. Participants

This is a cross-sectional, multicentre study of 16 PLAN patients recruited at 8 paediatric and 1 adult neurology departments in Spain and Portugal from January 2014 to September 2017. We included patients harbouring pathogenic mutations in *PLA2G6* in both alleles. Participants were assessed at the referral centres or at the coordinator centre, some of them during the first NBIA Spanish family meeting that took place on November 2015 (http://www.guiametabolica.org/noticia/primer-encuentro-asociacion-enach-espanola) following a standardised protocol. A questionnaire of 66 items comprising the age at onset of the main clinical signs and symptoms, and neurophysiological investigations, was completed in collaboration with the referral physician by retrospective analysis of medical records. In total, 16 patients were evaluated with this questionnaire, including two patients who were dead at the time of recruitment. All participants or their legal guardians provided informed consent for their participation/inclusion in the study. All procedures followed the Helsinki Declaration of 1975, as revised in 2000. The study was approved by the Ethic Committee at Sant Joan de Déu Hospital.

2.2. Neuroimaging

MRI obtained at Sant Joan de Déu were performed on a 1.5T MR scanner scan (Signa Excite, GE, Milwaukee, WI, USA) and included a sagittal or 3D-T1-weighted, axial T2-weighted and FLAIR, diffusion and SWI (susceptibility weighted imaging). Regarding brain MRI studies performed in other institutions (8 different institutions from Spain and Portugal) we accepted all the studies including at least T1-weighted sagittal, T2, FLAIR, diffusion weighted images in the axial and coronal planes, and any sequences sensitive to brain iron (T2*-/Gradient-Recalled Echo or/Susceptibility Weighted Imaging). MRI studies were systematically reviewed by three paediatric neurologists and two paediatric neuroimaging experts in consensus, the latter with more than 15 years of experience. Architecture and signal intensity of the cerebral hemispheres, corpus callosum, optic tracts, cerebellum, brainstem and basal ganglia were evaluated. Cerebellar atrophy was determined qualitatively as a small cerebellar volume and widening of the foliae. We measured the antero-posterior dimension of the medulla at the level of the clava on mid-sagittal T1-weighted images [11,12]. Furthermore, the relative size of the vermis was assessed using the midsagittal vermis relative diameter (MVRD), which was calculated as the ratio of the vermis size over the total posterior cranial fossa size [13]. These results were compared with fifteen age-matched controls that underwent examinations for seizures and headache. A child neuroradiologist ruled out morphologic abnormalities, and MRIs were interpreted as normal. The MRI evaluation sheet is described in Supplementary Table 1.

We also performed a systematic review of MRI abnormalities in *PLA2G6* patients by searching MEDLINE (through PubMed) using the following keywords: #1 PLA2G6, #2 infantile neuroaxonal dystrophy or #3 PLA2G6-associated neurodegeneration, combined with #4 magnetic resonance imaging. We selected a total of 12 articles that analysed MRI abnormalities in 164 patients with genetically confirmed PLAN.

2.3. Genetic analysis

Mutational screening of the *PLA2G6* gene was performed by Sanger sequencing of the codified exons and intronic flanking regions on an ABI Prism 3130XL analyzer (Applied Biosystems, Foster City, CA, USA). Once a variant was identified, all available first-degree family members were sequenced to identify the variant. The following databases were consulted to identify changes previously described: 1000G (http://www.internationalgenome.org/), ESP6500(http://evs.gs.washington.edu/EVS/), ClinVAR (https://www.ncbi.nlm.nih.gov/clinvar/), and HGMD (http://www.hgmd.cf.ac.uk/ac/index.php). Conservation of the residues was analysed using Clustal Omega (http://www.ebi.ac.uk/Tools/msa/clustalo/) and the pathogenicity was predicted using SIFT (http://sift.bii.a-star.edu.sg/), PolyPhen-2 (http://genetics.bwh.harvard.edu/pph2/) and PROVEAN (http://provean.jcvi.org/index.php) algorithms.

2.4. Neuropathology

A post-mortem neuropathologic brain examination was performed in P1 (see Table 1). The sections were paraffin-embedded, and thin sections were stained with haematoxylin and eosin, Perl's stain and Klüver-Barrera stain. Immunohistochemistry was performed using commercially available antibodies against glial fibrillary acidic protein (PGFA), ubiquitin, neurofilaments, tau and α-synuclein.

Table 1
Main clinical and neuroimaging data of the 16 patients of the cohort.

Pt	Onset/ Gait loss (y)	Clinical features								Neuroimaging			Variants
		Axial Hypotonia	Spasticity	Neuropathy	Epilepsy	Dystonia	Parkinsonism	Bulbar Dysfunction	Ophthalmological findings	Cerebellar Atrophy	Iron deposition	Other findings	Nucleotide Change 1/2
Infantile PLAN phenotype													
1†	1.8/4.7	+	+	+	+	+	–	+	N, VGP	Moderate	Pallidum/ SN	Cerebral atrophy,T2/FLAIR hyperintense putamen, optic atrophy	c.1626T > A(#)/c.1903C > T
2†	1.3/1.3	+	+	+	+	–	–	+	N	Moderate	No	Clava hypertrophy, thin/elongated corpus callosum	c.1547_1548dupCG/ c.1547_1548dupCG
3	1.2/2	+	+	+	–	–	–	+	N, OA, S	Moderate	Pallidum/ SN	T2/FLAIR hypertense cerebellar cortex, cerebral atrophy,thin/ elongated corpus callosum	c.2221C > T/c.2370T > G
4	1.5/2.5	+	+	+	+	+	–	–	OA	Moderate	Pallidum/ SN	T2/FLAIR hypertense cerebellar cortex, cerebral atrophy, T2/FLAIR cerebral white matter abnormalities,thin/elongated corpus callosum,T2/FLAIR hyperintense putamen, T2 hyperintense dentate nucleus	c.2017C > T(#)/c.2017C > T(#)
5	1.5/NW	+	+	–	–	–	–	–	S	Mild	No	Clava hypertrophy	c.1547_1548dupCG/ c.1547_1548dupCG
6	1.5/NW	+	+	+	–	+	–	+	S, BSP	Moderate	No	Clava hypertrophy	c.680C > T/c.680C > T
7	1.5/NW	+	+	+	–	+	–	+	N, BSP	Moderate	No	T2/FLAIR hypertense cerebellar cortex, T2 hyperintense dentate nucleus	c.680C > T/c.680C > T
8	0.7/NW	+	+	+	+	+	–	+	OA, S	Moderate	No	T2/FLAIR hypertense cerebellar cortex, clava hypertrophy, T2 hyperintense dentate nucleus	c.1903C > T/c.1903C > T
9	1.5/1.5	+	+	–	+	–	–	–	N, OA, S, BSP	Mild	No	Clava hypertrophy	c.2370T > G/c.2370T > G
10	1/1	+	+	+	–	+	–	+	N, OA, BSP	Moderate	No	Clava hypertrophy, T2/FLAIR hypertense cerebellar cortex, optic atrophy	c.221C > T/c.221C > T
Childhood PLAN phenotype													
11	3/5.5	+	+	–	+	+	+	+	OA, S	Moderate	Pallidum/ SN		c.1640A > G/c.1640A > G
12†	1/NW	+	+	–	+	+	–	+	–	NA	NA	NA	c.1435C > G(#)/c.2221C > T
13	1/22	+	+	–	+	+	+	+	BSP, VGP	Mild	Pallidum/ SN	Thin/elongated corpus callosum	c.1435C > G(#)/c.2221C > T
14	2/13	–	+	+	–	–	+	+	N, OA, S,BSP,VGP	Moderate	Pallidum/ SN	Clava hypertrophy, T2 hyperintense dentate nucleus	c.1027G > A/c.1010T > A(#)
15	4/10	+	+	–	–	–	–	+	N	Mild	Pallidum/ SN		c.1640A > G/c.1640A > G
16	4/8	+	+	–	–	–	–	–	–	Mild	Pallidum/ SN		c.1640A > G/c.1640A > G

ANAD: atypical neuroaxonal dystrophy. BSP: broken-up smooth pursuit. N: nystagmus. NA: not available. NW: Never walked. OA: optic atrophy. Pt: Patient. S: strabismus. SN: substantia nigra. VGP: vertical gaze palsy. (#) Novel mutations. † deceased.

2.5. Statistical analysis

Data analyses were conducted using the SPSS v.24.0 statistical package. Means, standard deviations, median, interquartile ranges and total ranges were computed for patient's data. Differences were reported as significant at $p < 0.05$. Based on the small sample size, Spearman's coefficients were calculated to search for correlations between MRI and clinical continuous variables. Categorical variables were analysed using the chi-squared test. The Mann-Whitney *U* test was used to compare continuous variables between two genetically different groups of patients: patients harbouring missense variants versus patients with nonsense and frameshift variants.

3. Results

3.1. Patients

Sixteen patients from 13 families were genetically diagnosed with PLAN. They were classified as infantile onset PLAN (n = 10) and childhood onset PLAN (n = 6). Four patients (P6, P7, P12 and P13) have been previously reported [14,15]. There were three pairs of siblings (P6-7; P12-13; P15-16), and one of them was twins (P6-7). Two patients were dead at the time of recruitment following status dystonicus (P1) and respiratory infection (P12). Moreover, P2 died during the study period from respiratory failure.

Almost all individuals were born after a normal pregnancy and had a normal perinatal history, except for two premature twin siblings (gestational age: 32 weeks) born after *in vitro* fertilisation. All patients had a normal early neurodevelopment, and ten patients had achieved independent gait before disease onset at a mean age of 1.8 years (range 0.8–4.0). The mean age at diagnosis was 8.8 years (range 2.7–30), and mean age at assessment was 10.2 years (range 3–33). Clinical data of the 16 patients is described in Table 1.

3.2. Neurological features

Fig. 1-a shows the prevalence of the main signs and symptoms in the 14 patients examined. All patients showed gait impairment, two patients could walk only with an accompanying person, whereas walking was impossible in the remaining 12 patients. Signs of axonal neuropathy were weakness, flaccidity, diminished or abolished reflexes, and muscle atrophy, and were later confirmed by nerve conduction and electromyography in all cases. Dystonia was present in distal upper or lower limbs (P8, P10, P11 and P13), trunk (P13), oromandibular region (P6, P7 and P10) and was generalised in one case (P4). Parkinsonism was represented by bradykinesia (P11, P13 and P14), rigidity (P11 and P13) and resting tremor (P13).

Fig. 1-b represents the chronological evolution of the disease in terms of age at onset of the main clinical features recorded by the questionnaire (n = 16).

3.3. Neuroimaging assessment

A total of 19 MRIs from 15 patients were analysed. Mean age at MRI was 4 years (range 1–22). The time frame between MRI acquisition and patient assessment was 1.7 ± 1.5 years (mean ± SD). Supplementary Table 2 summarises the neuroimaging abnormalities, and Fig. 2 shows the quantitative analysis performed and the main neuroimaging features in the cohort.

Cerebellar atrophy was present in all the neuroimaging studies (19/19), affecting both the vermis and cerebellar hemispheres in the majority of cases (16/19). Less frequent findings in the cerebellum and brainstem were the presence of clava hypertrophy (8/19) (Fig. 2-a), T2/FLAIR hyperintensity of the cerebellar cortex (6/19) (Fig. 2-b) and dentate nuclei (4/19) (Fig. 2-c).

Pallidum and substantia nigra T2 hypointensities were observed in 10/19 studies (mean age at MRI 10.2 ± 5 years) (Fig. 2-f, 2-g, 2-h and 2-i).

Quantitative analysis of the cerebellum showed that PLAN patients had a smaller MVRD than controls (0.62 ± 0.09 versus 0.83 ± 0.07, $p \leq 0,001$, Mann Whitney *U* Test). In four patients with more than one MRI, we selected the last study for correlation analysis of quantitative and clinical data. We found that MVRD correlated with the age at onset of relevant clinical variants (hypotonia, $r = 0.67$ $p = 0.047$; pyramidal signs, $r = 0.60$ $p = 0.027$; gait loss, $r = 0.66$ $p = 0.009$; Spearman's correlation), meaning that the earlier the onset of symptoms the more severe the cerebellar atrophy at the time of assessment. Clava size did not show any association with MVRD, dystonia or other clinical variables.

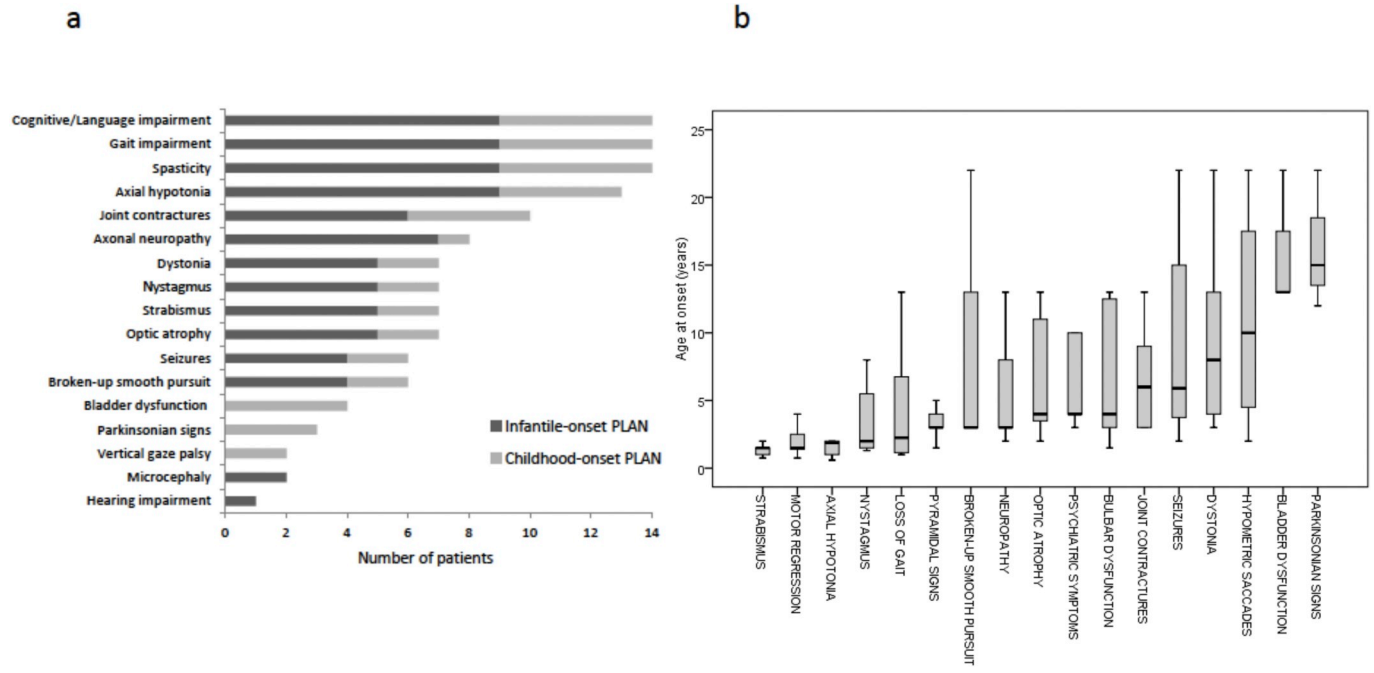

Fig. 1. Prevalence (a) and timing (b) of the main signs and symptoms in the study cohort.

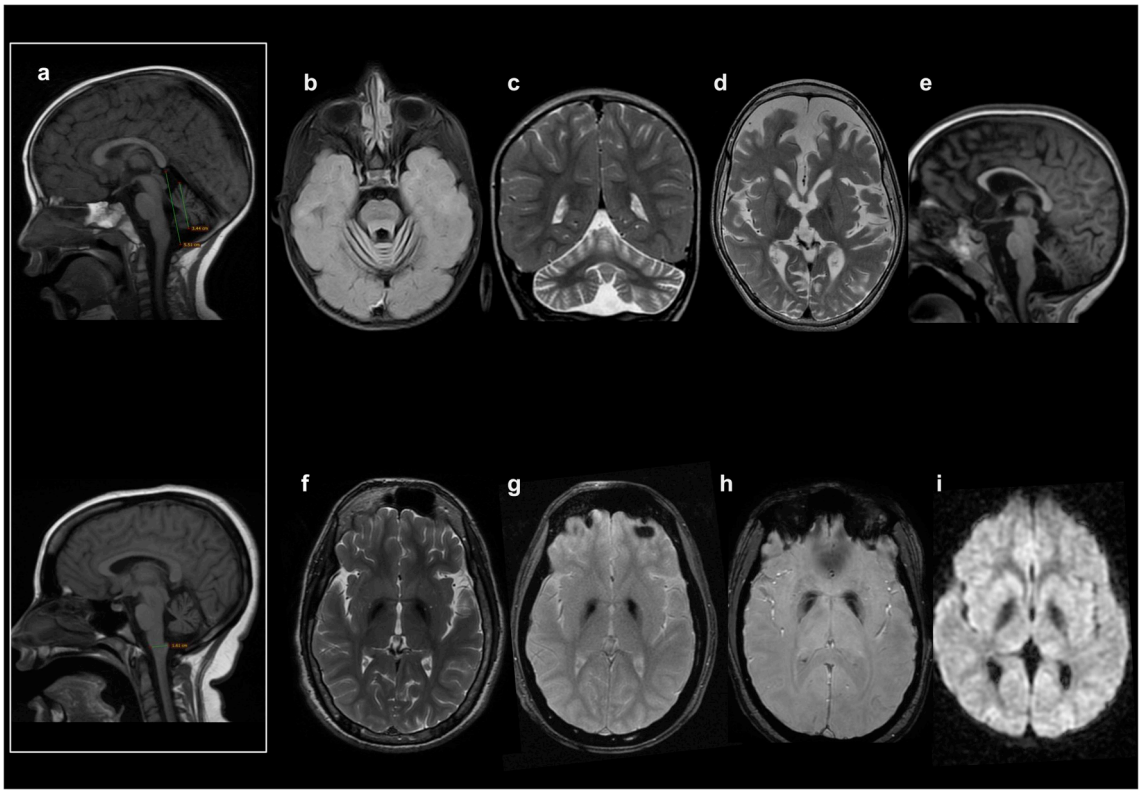

Fig. 2. Quantitative analysis and neuroimaging features. (a) Quantitative analysis: Midsagittal vermis relative diameter (MVRD) and clava size. MVRD was calculated using a midsagittal MR section and measuring total posterior cranial fossa diameter (a linear segment from the upper tentorium at the level of the posterior commissure to the occipital bone at the foramen magnum) and the largest axial diameter of the cerebellum parallel to the previous linear segment. The fraction (cerebellum diameter/total posterior cranial fossa diameter) is used to express the proportion of both values. The image represents MVRD calculation of patient 5, with MVRD result of 62% (P5, age 3 years). Clava size was measured using the anteroposterior dimension of the medulla at the level of the clava on midsagittal T1-weighted image (P14, age 14 years). (b) Axial FLAIR image demonstrating cerebellar cortical hyperintensity (Patient 10, age 3 years). (c) Coronal T2 weighted image demonstrating mild dentate nucleus hyperintensity and cerebellar atrophy characterised by widening of the foliae/fissures (Patient 8, age 2 years). (d) Axial T2 weighted image showing putamen hyperintensity, globus pallidus hypointensity and cerebral atrophy (Patient 4, age 9 years). (e) Midline sagittal T1 demonstrating predominantly inferior cerebellar vermian atrophy together with a thin and elongated corpus callosum (Patient 3, age 5 years). (f) Axial T2 weighted image and (g) axial T2* GRE image showing globus pallidus hypointensity, demonstrating iron deposition (Patient 11, age 13 years). (h) SWI image showing globus pallidus hypointensity (Patient 14, age 14 years). (i) Diffusion weighted image showing matching globus pallidus hypointensity (Patient 15, age 10 years).

Supplementary Table 3 summarises MRI data obtained from the literature review and our case series.

3.4. Molecular genetics

All patients had either homozygous or compound heterozygous mutations in the *PLA2G6* gene, including missense, nonsense and frameshift mutations (Supplementary Table 4). Four novel variants were identified (c.1626T > A; c.2017C > T; c.1435C > G; c.1010T > A) (http://espinos.cipf.es/index.php/en/mutations-db). To investigate the novelty of the variants, several databases were consulted (GnomAD, ClinVAR and professional HGMD). The remaining variants have been previously reported.

All the patients (n = 5) harbouring nonsense or frameshift mutations in both alleles were classified as infantile PLAN (Table 1 and Supplementary Table 4). On the other hand, patients with missense variants in both alleles were considered as childhood PLAN (n = 6) or infantile PLAN (n = 3). Patients with null mutations had an earlier age at onset of the main disease features than patients with missense variants in both alleles, although these differences did not reach statistical significance (disease onset: 1.3 ± 0.3 vs 2.2 ± 1.2; gait loss: 1.7 ± 1.6 vs 7.3 ± 7.7; pyramidal signs: 2.7 ± 1 vs 6 ± 3.8; axial hypotonia: 1.5 ± 0.7 vs 3.7 ± 5; dystonia 7.3 ± 2 vs 14.6 ± 11.3) (years). Further, MRI in null mutant patients was performed earlier (3.4 ± 3.2 vs 9.4 ± 6.4) showing smaller MVRD (0.57 ± 0.06 vs 0.63 ± 0.11). Again, these differences were not statistically significant (Supplementary Fig. 1).

Of note, a haplotype constructed on locus *PLA2G6* and a single nucleotide-based array analysis in the twin patients (P6-7) showed that both sisters had inherited most of the homologous chromosome 22 from their father, thus confirming uniparental disomy.[14] Supplementary Fig. 2 shows a schematic representation of *PLA2G6* and the location of the mutations identified in the present study.

3.5. Neuropathological findings

Autopsy from patient (P1), who died at 10 years of age, showed cerebral and cerebellar cortex atrophy, the latter affecting both vermian and hemispheric regions. Coronal sections showed brown coloured basal ganglia and substantia nigra. On microscopic investigation, the normal neocortical cerebellar hexalaminar architecture was variably disrupted by minimal spongiosis and neuronal loss (granular and Purkinje cells). Neuronal loss was also observed in the dentate nucleus. The basal ganglia showed gliosis with neuronal loss and mild spongiosis. Perl's staining showed iron-laden macrophages limited to the globus pallidi. Immunohistochemistry showed tau-positive granular inclusions in the neocortex. Granular deposits of ubiquitin were identified in the brainstem and basal ganglia, which were negative for α-synuclein. Neurofilament immunohistochemistry identified axonal spheroids, especially in the brainstem. The main neuropathological findings are shown in Fig. 3.

4. Discussion

This study delineates the spectrum and chronological evolution of the main neurological features in a cohort of 16 PLAN patients. Most patients presented with neurological regression within the first three years of life, following a period of normal development. Early signs, appearing before the age of five years, were oculomotor disorders, axial hypotonia, pyramidal signs, axonal neuropathy, gait impairment, optic atrophy, psychiatric symptoms and dysphagia. In contrast, later signs were joint contractures, seizures, dystonia, hypometric saccades, bladder dysfunction and parkinsonism [1,2,9,16,17].

Dystonia was found in almost half of the cohort, including both infantile and childhood onset PLAN patients. Dystonia varied from focal to generalised forms, and led to dystonic status and early death in one infantile onset PLAN patient. Dystonia was reported with variable frequency in previous series [2,9]. Further, status dystonicus is a rare feature described in PLAN [18].

All our patients showed cognitive and language regression after a period of normal development. Global language involvement and speech difficulties were prominent, especially dysartria/anarthria. A multifactorial origin was assumed, including oromandibular dystonia, corticobulbar and cerebellar dysfunction, and impaired brain development. Speech impairment is particularly prominent in NBIA disorders and other neurometabolic and neurodegenerative conditions leading to basal ganglia involvement [19].

Uncommon signs overlapping with other NBIA disorders were bladder dysfunction, parkinsonism and vertical gaze palsy. They were exclusively reported in childhood PLAN patients during the second decade of life in our series. Bladder dysfunction has been consistently associated with mitochondrial protein-associated neurodegeneration (MPAN) in the context of spinal cord and neuroaxonal degeneration [20]. Also, parkinsonian signs and vertical gaze palsy are rare features in childhood PLAN, and more commonly described in pantothenate kinase-associated neurodegeneration (PKAN). Treatment with levodopa was initiated in a patient with parkinsonian features in our series, and mild positive effect was observed [3,14,21].

We have performed qualitative and quantitative assessments of MRI abnormalities in 15 PLAN patients. Cerebellar atrophy was a universal neuroimaging feature in our series, in full agreement with previous literature [2,9,12]. We observed T2/FLAIR-hyperintense cerebellar cortex in one third of the MRI assessed, a nonspecific sign that indicates cortical gliosis [22,23]. Clava hypertrophy was evident in less than a half of our MRI studies. Taken together, cerebellar atrophy in coexistence with cerebellar cortex hyperintensity and clava hypertrophy could help physicians recognise PLAN in an appropriate clinical setting.

We performed quantitative analysis of the clava and the vermis size in order to test the hypothesis that these measurements could have any relationship with relevant clinical variables. Regarding clava size, no associations were observed. Clava hypertrophy has been associated with the presence of spheroid bodies on histopathology in some PLAN series, and its measurement has been validated [12]. The vermis size was measured using the MVRD, a bidimensional method previously used to correlate cerebellar atrophy with ataxia in PMM2-CDG patients [13]. We found that *PLA2G6* patients showed smaller MVRD than control patients, but higher values when compared with PMM2-CDG patients (data not shown) [13]. The MVRD is an easy and reproducible measurement that can be used when volumetric studies are not possible. However, it does not cover the involvement of the cerebellar hemispheres which was present in the majority of our MRI studies. Interestingly, we observed a significant correlation between the relative vermis size and the age at onset of axial hypotonia, pyramidal signs and gait loss, meaning that the earlier the onset of symptoms, the more severe the cerebellar atrophy. Further, we also observed that patients with null mutations in both alleles had smaller vermis size than patients with missense variants, although these differences were not significant, probably due to the small sample size.

The following sequences sensitive to brain iron (T2*-/Gradient-Recalled Echo or/Susceptibility Weighted Imaging) were useful to define the low signal within globus pallidum and substantia nigra, which was strikingly uniform and prominent in 57% of our patients, both infantile and childhood-onset PLAN patients. Iron accumulation did not show any association with the quantitative MRI measurements, the presence of dystonia or other clinical variables.

Anecdotal neuroimaging findings in our cohort were abnormal signal in the dentate nuclei, thin or elongated corpus callosum, cerebral atrophy, cerebral white matter abnormalities and putamen T2/FLAIR-hyperintensity [2,9,16]. Interestingly, an infantile PLAN patient developed microcephaly and severe cerebral atrophy (Fig. 2-d), both uncommon features in PLAN [8].

All the patients in our series had either homozygous or compound heterozygous mutations in the *PLA2G6* gene, including missense, nonsense and frameshift mutations. The 4 novel *PLA2G6* mutations

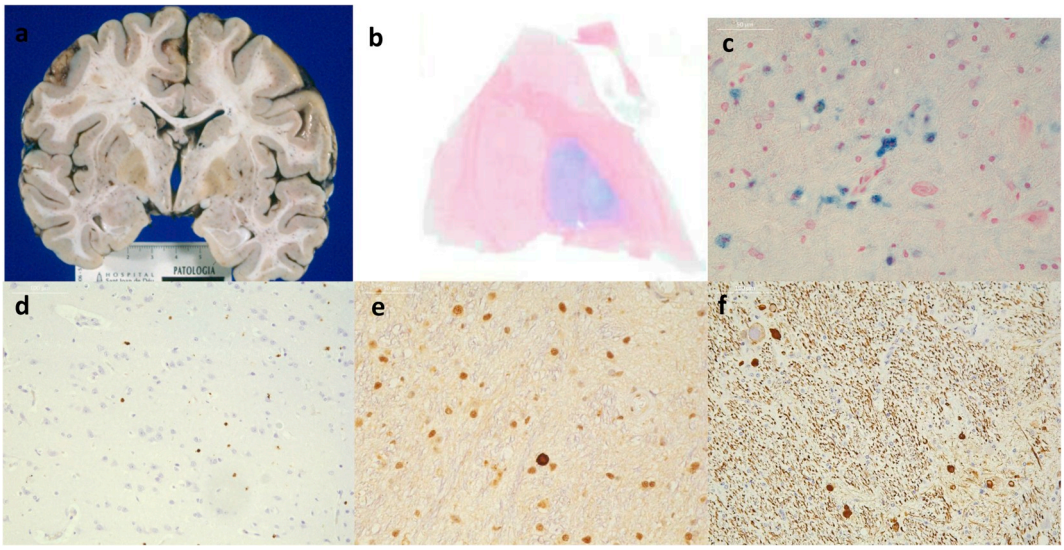

Fig. 3. Neuropathological abnormalities in a PLAN patient. a) Coronal macroscopic image of the brain, showing cerebral atrophy and browned coloured basal ganglia. b) Coronal section of the basal ganglia showing iron deposition in the globus pallidum (Perl's staining). c) Microscopic section of the globus pallidum showing iron-laden macrophagic cells. d) Immunohistochemistry for tau showing isolated deposits in the neocortex. e) Immunohistochemistry for ubiquitin showing positive bodies in the basal ganglia. f) Immunohistochemistry for neurofilaments showing axonal spheroids in the brainstem.

reported further expand the spectrum of variants associated with PLAN. Despite the failure to establish a clear genotype-phenotype correlation, our series coincides with published data showing that patients with null mutations manifested with clinical features earlier in life and developed more severe clinical phenotypes [2,6]. However, intra-familial phenotypic variability suggests that, apart from the type of mutations, other environmental and epigenetic factors may be implicated in disease pathogenesis [4,5].

Similar to previous reports, we observed the presence of axonal spheroids and iron deposition within the brain of an early dead infantile-onset PLAN child [2,8]. Depletion of cerebellar cortical neurons accompanied by marked astrocytosis was also detected in the cerebellum. Tau pathology was present in the neocortex of our patient, but not alpha-synuclein or positive Lewy bodies. Hyperphosphorylated tau accumulation has been described in PLAN and may be a common feature with other neurodegenerative diseases. Also, diffuse cortical and limbic alpha synuclein Lewy pathology, spheroids, brain iron accumulation, and cerebellar involvement are characteristic of PLA2G6 disorder [8,24].

This study has some limitations. Regarding the subjects of the study, the small sample size hampered establishing correlations between clinical and radiological variables among patients with different mutations. Also, our cohort did not represent the entire spectrum of PLA2G6-associated neurodegeneration, as we did not include adult forms (i.e. dystonia-parkinsonism phenotype). With respects to MRI assessment, PLAN patients were compared with controls that were not healthy subjects, despite the fact that neuroimaging in these cases was strictly normal. Moreover, we used a quantitative method that quantified the vermis size but not the cerebellar hemispheres, which were involved in the majority of the cohort. The volumetric analysis of the cerebellum, which is the gold standard to measure cerebellar volume, might overcome these limitations in future studies.

In conclusion, this study includes a systematic analysis of clinical features, disease progression, and biometric assessment of neuroimaging abnormalities in patients with infantile and childhood PLAN. We have identified early key clinical features that may help establish an early diagnosis. Also, we describe overlapping signs with other NBIA disorders that appear later probably related to the axonal and nigrostriatal degeneration. Cerebellar atrophy was the main radiological finding and correlated with the severity of the phenotype. Iron accumulation within the globus pallidum and substantia nigra was also a common and strikingly uniform sign regardless of the phenotype. Finally, we have described 4 previously unreported *PLA2G6* variants and identified uniparental disomy as a relevant inheritance mechanism, further confirming the importance of parental carrier testing in predicting the recurrence risk for families in this genetic defect.

Author contributions

Conceived and designed the study: BPD, AD.
Performed the genetic tests and its analysis: CE, CAT, VL.
Analysis and interpretation of data: BPD, AD, SAA, CE, CAT, VL.
Neuroimaging: AP, TAGMH, SAA, JM, MS, AD, BPD.
Neuropathology: CJM.
Wrote the paper/first draft: AD, BPD.
Statistical Analysis: AD, BPD.
Provided blood samples, data acquisition and clinical details of patients: AD, BPD, SAA, MS, MTV, RCL, JFR, AJE, PP, MOC, CO, AN, RCFM, MM, LA, SR, CG, TT, HGM.
All the authors have critically reviewed the manuscript.

Financial disclosures

Authors report no disclosures.

Acknowledgements

This work was supported by a grant from Fundació la Marató de TV3 (Grant no. 20143130 to BPD and 20143131 to CE), grant FIS PI15/00287 from the Plan Nacional de I + D + I and Instituto de Salud Carlos III- Subdirección General de Evaluación y Fomento de la Investigación Sanitaria". We thank the Spanish NBIA (ENACH) association, as well as the patients and their families for their collaboration in this study. We are grateful to the "Biobanc del Hospital Infantil Sant Joan de Déu per a la Investigació" member of the Spanish Biobank Network of ISCIII for the patient serum sample and data procurement.

Appendix A. Supplementary data

Supplementary data to this article can be found online at https://doi.org/10.1016/j.parkreldis.2018.10.013.

References

[1] A. Gregory, S. Hayflick, Neurodegeneration with brain iron accumulation disorders overview, 1993-2017, in: R.A. Pagon, M.P. Adam, H.H. Ardinger, S.E. Wallace, A. Amemiya, L.J.H. Bean, T.D. Bird, N. Ledbetter, H.C. Mefford, R.J.H. Smith, K. Stephens (Eds.), GeneReviews® [Internet], University of Washington, Seattle, Seattle (WA), 2013 Feb 28[updated 2014 Apr 24].
[2] A. Gregory, S.K. Westaway, I.E. Holm, P.T. Kotzbauer, P. Hogarth, S. Sonek, et al., Neurodegeneration associated with genetic defects in phospholipase A(2), Neurology 71 (18) (2008) 1402–1409.
[3] C. Paisán-Ruiz, K.P. Bhatia, A. Li, D. Hernandez, M. Davis, N.W. Wood, et al., Characterization of PLA2G6 as a locus for dystonia-parkinsonism, Ann. Neurol. 65 (1) (2009 Jan) 19–23.
[4] M. Synofzik, T. Gasser, Moving beyond Syndromic Classifications in Neurodegenerative Disease: the Example of PLA2G6. Movement Disorders Clinical Practice, Wiley InterScience, 2016 Published online 10 December 2016 www.interscience.wiley.com.
[5] B. Ozes, N. Karagoz, R. Schüle, A. Rebelo, M.J. Sobrido, F. Harmuth, M. Synofzik, et al., PLA2G6 mutations associated with a continuous clinical spectrum fron neuroaxonal dystrophy to hereditary spastic paraplegia, Clin. Genet. 92 (5) (2017) 534–539.
[6] N.V. Morgan, S.K. Westaway, J.E. Morton, A. Gregory, P. Gissen, S. Sonek, et al., PLA2G6, encoding a phospholipase A2, is mutated in neurodegenerative disorders with high brain iron, Nat. Genet. 38 (2006) 752–754.
[7] J. Balsinde, M.A. Balboa, Cellular regulation and proposed biological functions of group VIA calcium-independent phospholipase A2 in activated cells, Cell. Signal. 17 (2005) 1052–1062.
[8] C. Paisán-Ruiz, A. Li, S.A. Schneider, J.L. Holton, R. Johnson, D. Kidd, et al., Widespread Lewy body and tau accumulation in childhood and adult onset dystonia-parkinsonism cases with PLA2G6 mutations, Neurobiol. Aging 33 (4) (2012) 814–823.
[9] M.A. Kurian, N.V. Morgan, L. MacPherson, K. Foster, D. Peake, R. Gupta, et al., Phenotypic spectrum of neurodegeneration associated with mutations in the PLA2G6 gene (PLAN), Neurology 70 (18) (2008) 1623–1629.
[10] S. Karkheiran, G.A. Shahidi, R.H. Walker, C. Paisán-Ruiz, PLA2G6-associated dystonia-parkinsonism: case report and literature review, Tremor Other Hyperkinet. Mov. (N.Y.) 5 (2015) 317.
[11] S.I. Blaser, M. Steinlin, A. Al-Maawali, G. Yoon, The pediatric cerebellum in inherited neurodegenerative disorders: a pattern-recognition approach, Neuroimaging Clin. 26 (3) (2016) 373–416.
[12] A. Al-Maawali, G. Yoon, A.S. Feigenbaum, B.L. Banwell, D. Chitayat, S.I. Blaser, Validation of the finding of hypertrophy of the clava in infantile neuroaxonal dystrophy/PLA2G6 by biometric analysis, Neuroradiology 58 (10) (2016) 1035–1042.
[13] M. Serrano, V. de Diego, J. Muchart, D. Cuadras, A. Felipe, A. Macaya, et al., Phosphomannomutase deficiency (PMM2-CDG): ataxia and cerebellar assessment, Orphanet J. Rare Dis. 10 (2015) 138.
[14] P. Pérez-Torre, A. Escobar Villalba, P. Martínez Ulloa, M. Kawiorski, Jimenez-Escrig, E. Bazan, R. Gonzalo-Gobernado, et al., PLA2G6-Associated neurodegeneration: report of a novel mutation in two siblings with strikingly different clinical presentation, Mov. Dis. Clin. Pract. 4 (1) (2017) 129–131.
[15] C. Tello, A. Darling, V. Lupo, C.I. Ortez, B. Pérez-Dueñas, C. Espinós, Twin-sisters with PLA2G6-associated neurodegeneration due to paternal isodisomy of the chromosome 22 following in vitro fertilization, Clin. Genet. 92 (1) (2017) 117–118.
[16] A.O. Khan, A. AlDrees, S.A. Elmalik, H.H. Hassan, M. Michel, G. Stevanin, et al., Ophthalmic features of PLA2G6-related paediatric neurodegeneration with brain iron accumulation, Br. J. Ophthalmol. 98 (7) (2014) 889–893.
[17] N. Nardocci, G. Zorzi, L. Farina, S. Binelli, W. Scaioli, C. Ciano, et al., Infantile neuroaxonal dystrophy: clinical spectrum and diagnostic criteria, Neurology 52 (1999) 1472–1478.
[18] L. Cif, M.A. Kurian, V. Gonzalez, S. Garcia-Ptacek, T. Roujeau, P. Gelisse, et al., Atypical PLA2G6-associated neurodegeneration: social communication impairment, dystonia and response to deep brain stimulation, Mov. Disord. Clin. Pract. 1 (2014)

128–131.
[19] C. Ganos, B. Crowe, M. Stamelou, N. Kresojevi, M.J. Luki, J. Bras, R. Guerreiro, et al., The clinical syndrome of dystonia with anarthria/aphonia, Park. Relat. Disord. 24 (2016) 20–27.
[20] P. Hogarth, A. Gregory, M.C. Kruer, L. Sanford, W. Wagoner, M.R. Natowicz, et al., New NBIA subtype: genetic, clinical, pathologic, and radiographic features of MPAN, Neurology 80 (2013) 268–275.
[21] R.A. Egan, R.G. Weleber, P. Hogarth, A. Gregory, J. Coryell, S.K. Westaway, et al., Neuro-ophthalmologic and electroretinographic findings in pantothenate kinase-associated neurodegeneration (formerly Hallervorden-Spatz syndrome), Am. J. Ophthalmol. 140 (2) (2005) 267–274.
[22] N.I. Wolf, M. Koenig, Progressive cerebellar atrophy: hereditary ataxias and disorders with spinocerebellar degeneration, Handb. Clin. Neurol. 113 (2013) 1869–1878.
[23] T. Bosemani, G. Zanni, A. Hartman, R. Cohen, T.A. Huisman, E. Bertini, et al., Christianson syndrome: spectrum of neuroimaging findings, Neuropediatrics 45 (4) (2014) 247–251.
[24] S. Schneider, R. Alcalay, Neuropathology of genetic synucleinopathies with parkinsonism: review of the literature, Mov. Disord. 32 (11) (2017) 1504–1523.